Received: 1 June 2021 | Revised: 24 September 2021 | Accepted: 10 October 2021

DOI: 10.1002/nbm.4643

RESEARCH ARTICLE

NMR IN BIOMEDICINE WILEY

Myocardial blood flow is the dominant factor influencing cardiac magnetic resonance adenosine stress T2

Jill J. Weyers[1] | Venkat Ramanan[1] | Ahsan Javed[2] | Jennifer Barry[1] | Melissa Larsen[1] | Krishna Nayak[2] | Graham A. Wright[1,3,4] | Nilesh R. Ghugre[1,3,4]

[1]Physical Sciences Platform, Sunnybrook Research Institute, Toronto, Ontario, Canada

[2]Ming Hsieh Department of Electrical Engineering, University of Southern California, Los Angeles, California

[3]Schulich Heart Research Program, Sunnybrook Health Sciences Centre, Toronto, Ontario, Canada

[4]Department of Medical Biophysics, University of Toronto, Toronto, Ontario, Canada

Correspondence
Jill Weyers, Physical Sciences Platform, Sunnybrook Research Institute, 2075 Bayview Ave Rm M7-508, Toronto, Ontario, Canada M4N 3M5
Email: jweyers@sri.utoronto.ca

Nilesh Ghugre, Physical Sciences Platform, Sunnybrook Research Institute, 2075 Bayview Ave Rm M7-510, Toronto, Ontario, Canada M4N 3M5
Email: nghugre@sri.utoronto.ca

Present address
Ahsan Javed, Cardiovascular Branch, Division of Intramural Research, National Heart, Lung, and Blood Institute, National Institutes of Health, Bethesda, Maryland

Funding information
Heart and Stroke Foundation of Canada; Heart and Stroke Foundation of Ontario; National Institutes of Health; Ontario Research Fund

Stress imaging identifies ischemic myocardium by comparing hemodynamics during rest and hyperemic stress. Hyperemia affects multiple hemodynamic parameters in myocardium, including myocardial blood flow (MBF), myocardial blood volume (MBV), and venous blood oxygen levels (PvO_2). Cardiac T2 is sensitive to these changes and therefore is a promising non-contrast option for stress imaging; however, the impact of individual hemodynamic factors on T2 is poorly understood, making the connection from altered T2 to changes within the tissue difficult. To better understand this interplay, we performed T2 mapping and measured various hemodynamic factors independently in healthy pigs at multiple levels of hyperemic stress, induced by different doses of adenosine (0.14-0.56 mg/kg/min). T1 mapping quantified changes in MBV. MBF was assessed with microspheres, and oxygen consumption was determined by the rate pressure product (RPP). Simulations were also run to better characterize individual contributions to T2.

Myocardial T2, MBF, oxygen consumption, and MBV all changed to varying extents between each level of adenosine stress (T2 = 37.6-41.8 ms; MBF = 0.48-1.32 mL/min/g; RPP = 6507-4001 bmp*mmHg; maximum percent change in MBV = 1.31%). Multivariable analyses revealed MBF as the dominant influence on T2 during hyperemia (significant β-values >7). Myocardial oxygen consumption had almost no effect on T2 (β-values <0.002); since PvO_2 is influenced by both oxygen consumption and MBF, PvO_2 changes detected by T2 during adenosine stress can be attributed to MBF. Simulations varying PvO_2 and MBV confirmed that PvO_2 had the strongest influence on T2, but MBV became important at high PvO_2. Together, these data suggest a model where, during adenosine stress, myocardial T2 responds predominantly to changes in MBF, but at high hyperemia MBV is also influential. Thus, changes in adenosine stress T2 can now be interpreted in terms of the physiological changes that led to it, enabling T2 mapping to become a viable non-contrast option to detect ischemic myocardial tissue.

KEYWORDS
adenosine stress, cardiac MRI T2 mapping, heart disease, myocardial blood flow, myocardial blood volume, stress imaging

Abbreviations: AHA, American Heart Association; BP, blood pressure; CMR, cardiac magnetic resonance; CV, coefficient of variation; HR, heart rate; MBF, myocardial blood flow; MBV, myocardial blood volume; MPR, myocardial perfusion reserve; PvO_2, percent venous oxygen; RPP, rate pressure product.

1 | INTRODUCTION

As heart disease remains the most common health problem worldwide, detecting and identifying ischemic myocardium is of increasing importance. One method for probing myocardial tissue is stress imaging, which reveals the change in various hemodynamic factors between rest and hyperemic stress, a state induced via vasodilators such as adenosine, regadenoson, or dipyridamole.[1–4] Stress imaging can detect pre-symptomatic stenoses,[5–8] and has been recognized as a successful predictor of major adverse cardiovascular events.[9,10] Currently, it is performed using several different imaging techniques, including first pass perfusion cardiac magnetic resonance (CMR),[11] positron emission tomography/single-photon emission computed tomography imaging,[12,13] computed tomography (CT) perfusion angiography,[14,15] and myocardial contrast echocardiography,[16] but unfortunately, these imaging techniques require radiation exposure and/or injection of a contrast agent or tracer. Given rising concerns about kidney toxicity,[17] radiation exposure,[18,19] and long-term retention of contrast agents,[20–23] the need for non-contrast methods of myocardial stress imaging is growing. CMR stress T2 relaxometry is a non-contrast method that allows the quantitative assessment of various tissue characteristics, and it may be able to fill this niche.

Hyperemic stress alters several hemodynamic factors, including myocardial blood flow (MBF), myocardial blood volume (MBV), blood pressure (BP), and myocardial workload, which in turn affects myocardial oxygen consumption. Myocardial T2 directly detects myocardial tissue fluid and blood oxygen levels,[24] but these parameters are each reflective of several tissue characteristics, many of which overlap with the changes that occur during hyperemia. Tissue fluid detected by T2 includes MBV as well as extracellular and intracellular fluid volumes,[25] but hyperemia-induced changes in tissue fluid are typically limited to MBV.[26] T2 detects blood oxygen levels via the paramagnetic effects of deoxyhemoglobin,[27,28] but, since arterial blood does not change oxygenation state under normal circumstances, variations in oxygen detected by T2 reflect changes in percent venous oxygen (PvO_2). PvO_2 is affected by both myocardial oxygen consumption and the rate of oxygen delivery, which is a function of MBF. Therefore, because T2 directly detects changes in tissue fluid and PvO_2, it is sensitive to multiple hyperemia-relevant hemodynamic factors. Indeed, T2 has been shown to be capable of detecting changes in MBF,[29–31] PvO_2,[24,25,32] and MBV,[24,29] and proven as a viable option for detecting ischemic myocardium.[33,34]

While the multifactorial nature of T2 makes it useful for detecting multiple individual stress-induced hemodynamic changes, interpreting stress T2 in terms of the overall tissue state during hyperemia is difficult; for example, T2 relaxation is increased by both higher tissue fluid and higher PvO_2.[24,25,29,32] Understanding the interplay between each hemodynamic factor and its individual influence on stress T2 is key to understanding how stress T2 reflects tissue changes. To address this, we evaluated T2 as well as MBF, MBV, and myocardial oxygen consumption during varying levels of adenosine-induced hyperemic stress. We then performed stress T2 simulations to better isolate the contribution of each physiological factor.

2 | EXPERIMENTAL METHODS

2.1 | Animal procedures

Animal procedures were approved by the Animal Care Committee of Sunnybrook Research Institute. Twelve healthy Yorkshire pigs (Caughell Farms, Fingal, ON, Canada), including both sexes (42% female) and a wide range of weights (32-110 kg), were used for this study; no fibrosis, hemorrhage, or edema were present in the myocardium to complicate tissue analysis. For all studies, pigs were sedated with either ketamine and atropine (33 mg/kg and 0.05 mg/kg, respectively) or dexmedetomidine (0.05-0.08 mg/kg), and intubated and mechanically ventilated with 2% oxygen and isoflurane ranging from 1 to 5%, as required to obtain surgical anesthesia. Virtually all coronary hemodynamic measurements were made with isoflurane doses between 2 and 3.5%. Dexmedetomidine was reversed with antisedan (0.05-0.08 mg/kg). For analgesia, pigs received tramadol (4 mg/kg) before surgeries, and Metacam (0.4 mg/kg IM) after survival procedures.

2.2 | Adenosine infusions

Four doses of adenosine were used: the "standard" human dose[35] (1×, 0.14 mg/kg/min), and double (2×, 0.28 mg/kg/min), triple (3×, 0.42 mg/kg/min), and quadruple the standard dose (4×, 0.56 mg/kg/min). Adenosine powder (A9251, Sigma, St. Louis, MO) was dissolved in saline at 3 mg/mL, filter sterilized (VWR, Radnor, PA, USA, 76010-404), and administered through an ear vein at the constant rate appropriate for each dose using an infusion pump. Each pig was assigned a dosing regimen with up to four doses of adenosine (Figure 1A), administered during both the CMR examination (Figure 1B) and the microsphere injection surgery (Figure 1C). Dose order was randomized for each pig to cancel out any potential biases due to previous doses or experimental timing. All procedures were executed under a strict time schedule to ensure that each measurement occurred at the same time point after the start of infusion from dose to dose and pig to pig, as per Figure 1. Once an infusion started, all procedures paused for 2 min to allow the hemodynamic effects to stabilize.

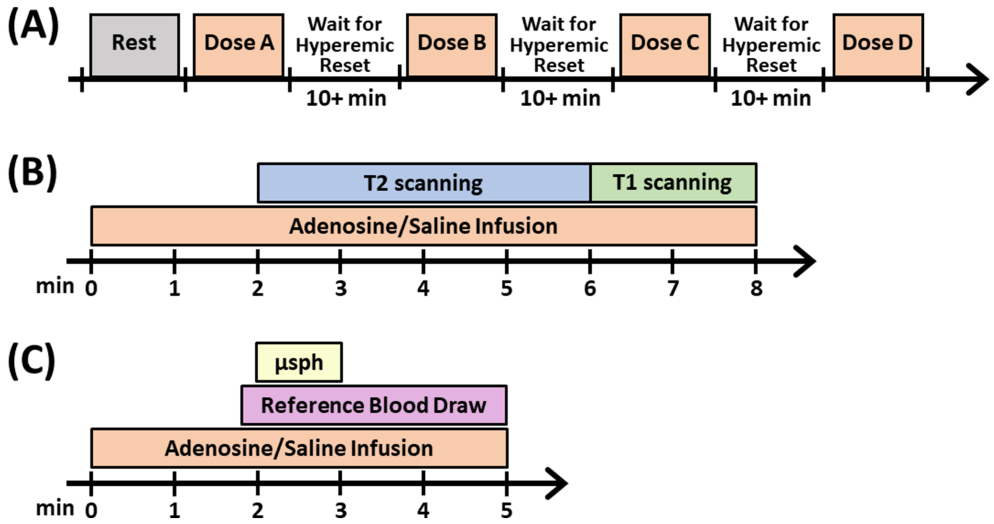

FIGURE 1 Experimental time courses of procedures involving adenosine infusions. A, Overall time course for testing multiple adenosine doses. B, C, The specific timing of each individual adenosine infusion (orange boxes in A) during either the CMR examination (B) or microsphere injection (C). "μsph" refers to the time period when microspheres were injected

2.3 | CMR scanning

Scanning was done in a horizontal whole body 3 T scanner (MR750, GE Healthcare, Milwaukee, WI). Animals were anesthetized and intubated as above and placed supine on the scanner table. An eight-channel cardiac coil array was placed on the animal's chest, and heart rate (HR) was monitored for prospective gating.

Scans began with localizers and cine acquisitions, followed by repeated rounds of T2 and T1 mapping with or without adenosine (Figure 1A and 1B). T2 maps were cardiac-gated to diastole and acquired during breath holds at five short axis slice locations spread from base to apex using a standard T2-prepared spiral acquisition scheme, as previously published.[33] Other settings were as follows: 10 interleaves (12.3 ms, 3072 points), T_E = 2.9, 24.3, 45.6, 88.2, and 184.2 ms, in-plane resolution ~ 1 mm, slice thickness = 5 mm, bandwidth = 125 kHz, field of view = 280 × 280 mm^2.

T1 maps were cardiac-gated to diastole and acquired during breath holds at the same short axis slice locations as T2 using a standard modified Look-Locker inversion recovery (MOLLI) sequence with a 6-6 pattern and a three or four heartbeat dead time to avoid HR dependence,[36] as previously published.[37] Other parameters were as follows: flip angle = 35°, matrix = 160 × 160, in-plane resolution = 1.75 mm, slice thickness = 5 mm, field of view = 280 × 280 mm^2.

2.4 | CMR analysis

CMR images were analyzed in CVI42 software (Circle Cardiovascular Imaging, Calgary, Alberta, Canada). T1 and T2 maps were produced in CVI42, excluding pixels of zero values. Contours were drawn manually with care to avoid artifacts as well as the blood pool and epicardial edge such that only the mid-myocardium was analyzed. Since there may have been subtle differences in the timing of gating and shape of the myocardium with each dose of adenosine, contours were redrawn for each dose. Each slice was divided into six segments according to American Heart Association (AHA) guidelines.[38] If artifacts were unavoidable, those segments were excluded from analysis. Most artifacts occurred in the inferolateral free wall, arising from susceptibility effects at the heart-lung interface.

2.5 | T2 simulations

Simulations are based on a two-pool model of fluid exchange, using algorithms, variables, and parameters derived and explained by Stainsby and Wright.[25] Simulations were run using custom MATLAB (MathWorks, Natick, MA) scripts, as previously described.[25,33,39] Echo time, field strength, and other varied parameters were matched to those used during scanning.

2.6 | Microsphere-based MBF measurements

Microsphere injection and tissue processing occurred via standard microsphere techniques, adapted from Glenny et al. and the Fluorescent Microsphere Resource Center.[40,41] CMR and microsphere procedures could not be performed simultaneously because microsphere injection involved equipment that is not MR-compatible. Moreover, the two procedures were not conducted sequentially to avoid overly long periods of anesthesia and related concerns of reduced hemodynamic response to adenosine. However, the two procedures were performed as close together as was practical (mean 8 d apart). Animals were anesthetized and intubated as above. A catheter was placed in the left ventricle for injection of fluoroscopy contrast and microspheres, and another was placed in the mid-descending aorta for reference blood withdrawal. 9×10^6 fluorescent microspheres (FluoSpheres, 15 μm, seven-color kit, F8891, Thermo Fisher, Waltham, MA) were sonicated and manually injected as per the timing in Figure 1C. Spectrally distinct microspheres were used for each round. Colors used were (with their excitation/emission maxima, nm) blue (365/415), blue-green (430/465), yellow-green (505/515), orange (540/560), red (580/605), crimson (625/645), and scarlet (645/680).

During microsphere injection, reference blood was collected via syringe pump into a 50 mL glass syringe (Hamilton Company, Reno, NV) preloaded with heparin (20 U/mL) and 50 μL of a unique color of microspheres (50 000 microspheres total) as an internal standard. After withdrawal, blood was stored in 50 mL sterile, amber glass vials (SEV50AMB, Farris Labs, Fort Worth, TX) at 4 °C. Between microsphere injections, all injection and collection lines were replaced to prevent cross-color contamination.

At the end of the procedure, the animal was sacrificed by intravenous injection of saturated potassium chloride (P9541, Sigma). The heart was resected, cannulated, and perfused with saline, adenosine, and 10% neutral buffered formalin for 30 min. The heart was then immersed in formalin and fixed for a minimum of 24 h.

2.7 | Tissue processing and microsphere quantification

Fixed hearts were manually sliced transaxially into slices about 5-7 mm thick using a trimming knife (F260P, Feather, Osaka, Japan). After slicing, the heart was reassembled and the distance from the apex to the middle of each slice was measured. Similar calculations were done using CMR slice locations, and two tissue slices corresponding to the location of two CMR slices were selected for microsphere quantitation. Most selected slices were mid-myocardial, corresponding to AHA segments 7-12, but to stay in line with the location of CMR slices they were occasionally more basally derived, corresponding to segments 1-6. Selected slices were cut into segments according to AHA guidelines[38] to extract and quantify microspheres. Reference blood and myocardial segments were digested in potassium hydroxide and vacuum filtered with Cyclopore polycarbonate filters (Whatman, 7060-2511, GE Healthcare, Chicago, IL). Filtrate was then dissolved in 2-ethoxyethyl acetate (109967, Sigma) and the fluorescent signal was read in a Synergy H1 plate reader (BioTek, Winooski, VT). Spectral overlap between colors was compensated for via matrix inversion, using a spreadsheet provided by the Fluorescent Microsphere Resource Center.[41] All samples were processed in duplicate and read in triplicate; results were averaged.

2.8 | Final analyses and statistics

Final analyses were done in Excel (Microsoft, Redmond, WA). Statistics and graphing were done in Prism (GraphPad, San Diego, CA). Statistical analyses comparing all groups were done by one-way ANOVA, with a Tukey post-test. In all graphs, error bars are SEM. Significance is reported as P values: $^*P \le 0.05$, $^{**}P \le 0.01$, $^{***}P \le 0.001$, and $^{****}P \le 0.0001$.

Multivariable linear regression was performed in Prism, Version 9.0.0. Segmental data were fit using a least squares method and incorporating two-way interactions between the rate pressure product (RPP) and MBF, since they are both components of PvO_2. The resulting model was of the form $y = \beta_0 + \beta_1 B + \beta_2 C + \beta_3 D + \beta_4 BC$, where y is the dependent variable (T2), and B, C, and D represent the RPP (reflecting oxygen consumption), MBF, and T1 (reflecting MBV), respectively. Each β is a weighting factor. Model fit was confirmed with Akaike's information criterion. Collinearity was reduced using centered data, which lowered all relevant variance inflation factors below 7.

3 | RESULTS

3.1 | Stress T2 response to various levels of hyperemia

We first determined how myocardial stress T2 changed in response to differing levels of hyperemic stress, induced using four different doses of adenosine. T2 maps revealed that myocardial T2 increased at each level of stress when compared with rest (<FIG 2>Figure 2A-F, <TAB 1>Table 1), with larger increases at higher doses of adenosine. The largest incremental dose-to-dose changes occurred at the 1× and 3× doses. The percent

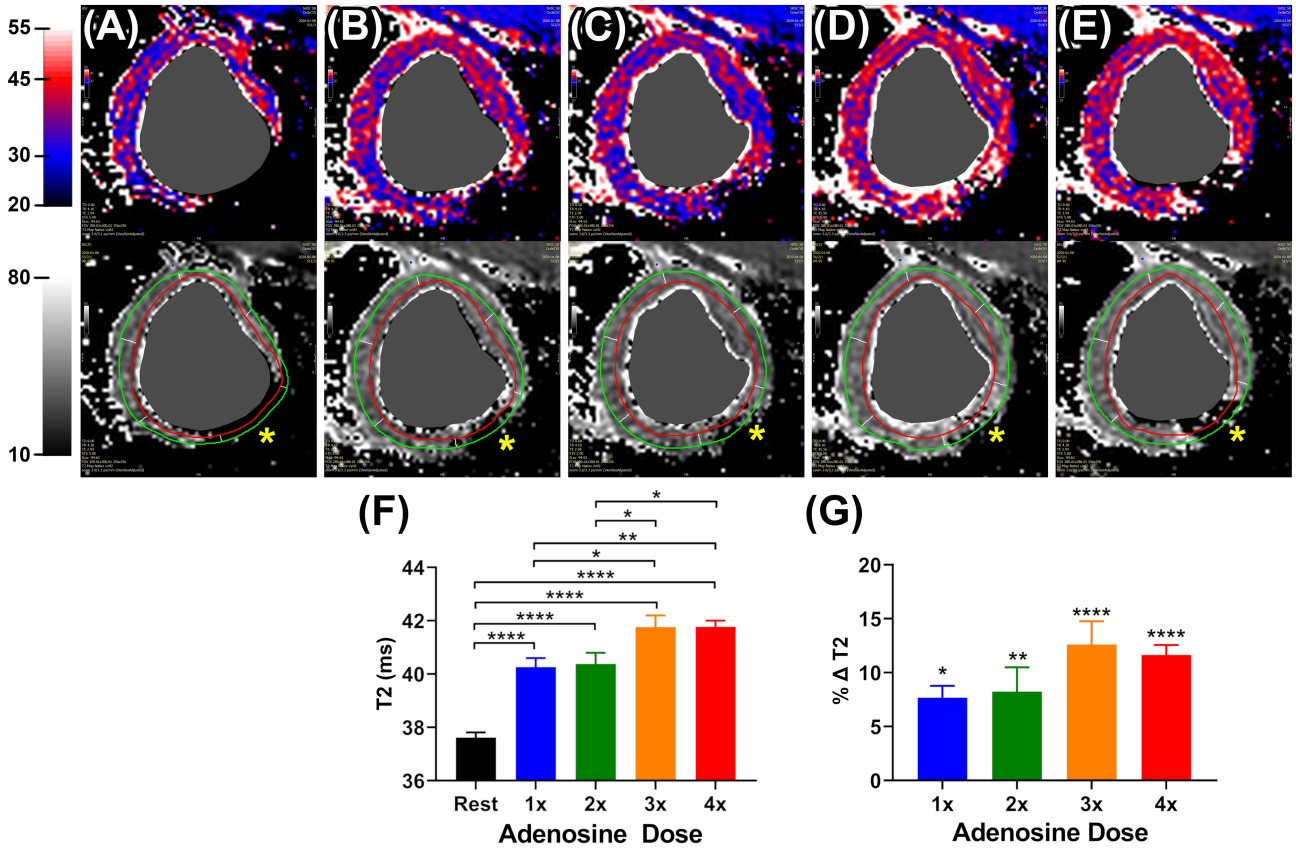

FIGURE 2 T2 increases at all levels of adenosine stress. A-E, T2 maps of the same heart at rest (A) and during a 1× (B), 2× (C), 3× (D), and 4× (E) dose infusion of adenosine, without (top) and with (bottom) contours. Pixels are false-colored as in the keys beside A. The blood pool was manually grayed out for clarity. Segments containing imaging artifacts (yellow asterisks) were excluded from analysis. F, G, Quantification of stress T2 (F) and percent change in stress T2 (G). Colored bars represent the average of myocardial segments. G, Significance is noted for each dose compared with no change

TABLE 1 Summary of hemodynamic measurements

	Rest	1× adenosine	2× adenosine	3× adenosine	4× adenosine
T2 (ms)	37.62 ± 2.66	40.26 ± 3.35 ****	40.38 ± 3.93 ****,#	41.76 ± 4.18 ****,#,$	41.77 ± 3.19 ****,##,$
Percent change T2	–	7.67 ± 5.29 *	8.24 ± 10.04 **	12.62 ± 9.79 ****	11.64 ± 6.28 ****
MBF (mL/min/g)	0.482 ± 0.255	0.834 ± 0.393 *	0.965 ± 0.706 **	1.320 ± 0.539 ****,##	0.941 ± 0.484 ****,##,&
MPR	–	1.44 ± 0.53	2.18 ± 0.48	3.10 ± 1.56 ####,$	2.59 ± 1.26 ###
Systolic BP (mmHg)	68 ± 16	67 ± 1	64 ± 9	51 ± 4	49 ± 15 *
HR (bmp)	98 ± 11	100 ± 5	95 ± 9	92 ± 8	81 ± 15 **,##,$
RPP (bmp*mmHg)	6507 ± 1821	6903 ± 385	5710 ± 783	4702 ± 796	4001 ± 1901 **,#
T1 (ms)	1148 ± 32	1142 ± 26	1151 ± 26	1159 ± 32 ##	1168 ± 25 ***,####,$$
Percent change T1	–	−0.88 ± 1.51	0.10 ± 1.61	0.93 ± 1.64 ##	1.31 ± 1.44 ###

Data is mean with standard deviation. Percent change is compared with rest values. Statistical significance is shown as follows: * compared with baseline, # compared with the 1× dose, $ compared with the 2× dose, & compared with the 3× dose.

change in T2 exhibited a similar pattern; however, the changes were not significant from dose to dose (Figure 2G, Table 1). Regardless, these results confirm that T2 was indeed sensitive to varying levels of hyperemia.

3.2 | Myocardial blood oxygenation during hyperemic stress

T2 directly detects PvO_2,[24] but PvO_2 is affected by both oxygen delivery and oxygen consumption. Therefore, to understand the changes in myocardial PvO_2 that occur during adenosine stress we measured oxygen delivery and oxygen consumption independently. Oxygen delivery corresponds to the MBF rate; increases in MBF increase myocardial PvO_2. Measured by microsphere injection, MBF increased with increasing adenosine in a nearly linear, dose-dependent manner up to the 3× dose, and then sharply decreased at the 4× dose (<FIG 3>Figure 3A, Table 1). Myocardial perfusion reserve (MPR), the ratio of stress perfusion over rest perfusion,[42,43] exhibited a similar pattern (Figure 3B, Table 1). Changes in both MBF and MPR were consistent across the entire myocardium (Supporting Figure S1).

Myocardial oxygen consumption is directly proportional to the rate-pressure product (RPP), the product of systolic BP and HR.[44] A decrease in the RPP means decreased oxygen consumption, which increases myocardial PvO_2. During adenosine infusions greater than the 1× dose both BP and HR dropped sharply within the first 90 s of the infusion and then stabilized into a steady decline, with HR displaying more dose dependence than BP (Supporting Figure 2). Correspondingly, there was almost no change in the RPP with the 1× dose of adenosine, but higher doses all caused a large decrease (<FIG 4>Figure 4, Table 1). The maximum percent changes in the RPP at doses higher than 1× were statistically different from values at rest; however, they were not significantly different from each other (Figure 4B).

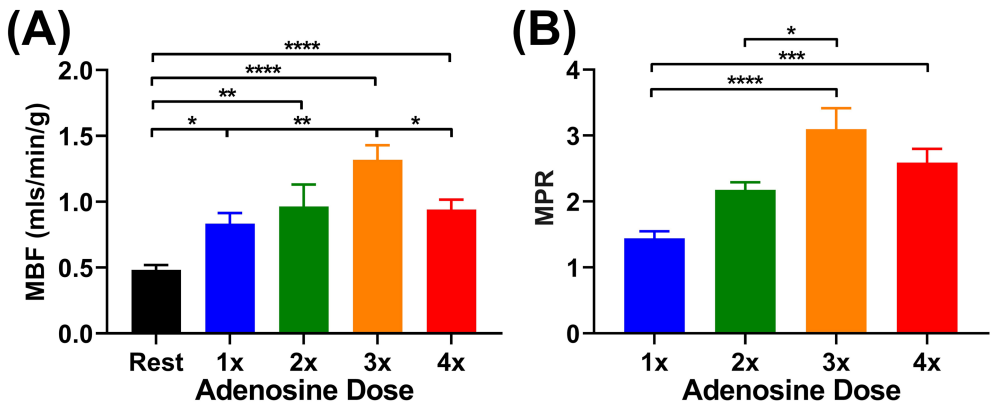

FIGURE 3 MBF increases with increasing adenosine until the 3× dose. Graphs quantifying MBF (A) or MPR (B). Bars represent the average of myocardial segments

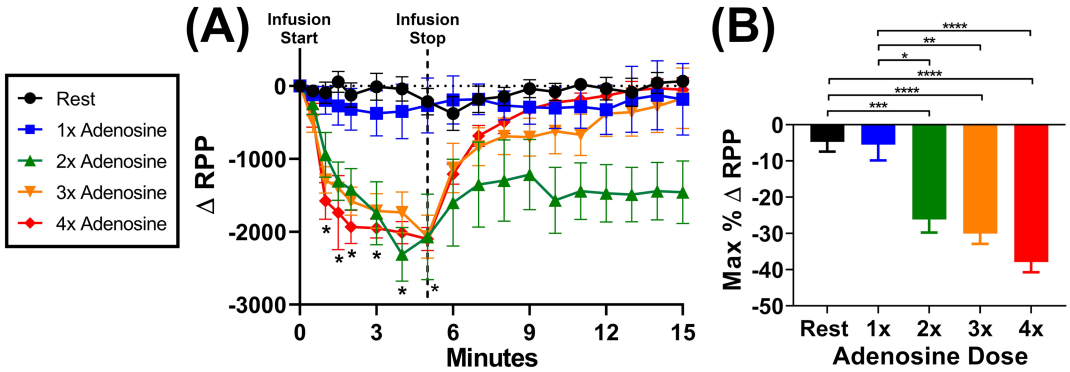

FIGURE 4 RPP drops in response to adenosine. Graph of the time course (A) and maximum percent change (B) of the RPP during 5 min infusions of varying adenosine doses. In the time course, measurements were made at 30 s intervals for the first 2 min, and at 1 min intervals thereafter. Asterisks in the timeline report significance from baseline, but do not specify the significant dose, while asterisks in the bar graph report level of significance. We note that, while the pattern of recovery in the 2× dose is idiosyncratic, none of the data points in this recovery period are statistically significantly different from one another, so we do not believe this is a biologically relevant event

3.3 | Myocardial tissue fluid during hyperemic stress

To measure the changes in myocardial fluid during each level of hyperemia we used stress T1 mapping, a measurement sensitive to fluid levels.[26] A rise in T1 is consistent with an increase in MBV.[26,45] T1 maps indicate changes in myocardial T1 between adenosine doses (<FIG 5>Figure 5A-E). Surprisingly, quantification of myocardial T1 as well as the percent change in T1 revealed a drop at the 1× dose (Figure 5F and 5G, Table 1). At the 2× dose there was little change from rest values, but higher adenosine doses induced dose-dependent increases in T1, as expected.

3.4 | Multivariable analysis between hemodynamic factors and stress T2

To determine the individual influences that MBF, oxygen consumption (via RPP), and MBV (via T1) each have on T2 during stress, we performed multivariable linear regression. Analysis incorporating data from all adenosine doses produced a model with a poor correlation coefficient ($R^2 = 0.097$, not shown), suggesting that a single model cannot explain T2 across all levels of hyperemia. Step-wise models incorporating changes at each level of hyperemia achieved much better correlations (Table 2). While the individual *P*-values of each β-value did not always reach significance, the overall trends indicate that MBF was the dominant factor affecting T2, though its effect waned at higher adenosine doses (Table 2). Oxygen consumption had negligible influence on T2 (all β values were smaller than 0.002). MBV had a small influence at all levels of hyperemia, though none of the MBV β-values reached significance.

3.5 | Stress T2 simulations to independently isolate the effects of MBV and PvO_2

To further explore the complex relationship between hemodynamic changes and stress T2 we ran simulations (validated in the Supporting Results and Supporting Figure 3) isolating the two factors that T2 directly detects: MBV and PvO_2. For the first series of simulations, PvO_2 was held constant to determine how changes in MBV alone impact stress T2. The output was dependent on the value of PvO_2 held constant, but in general

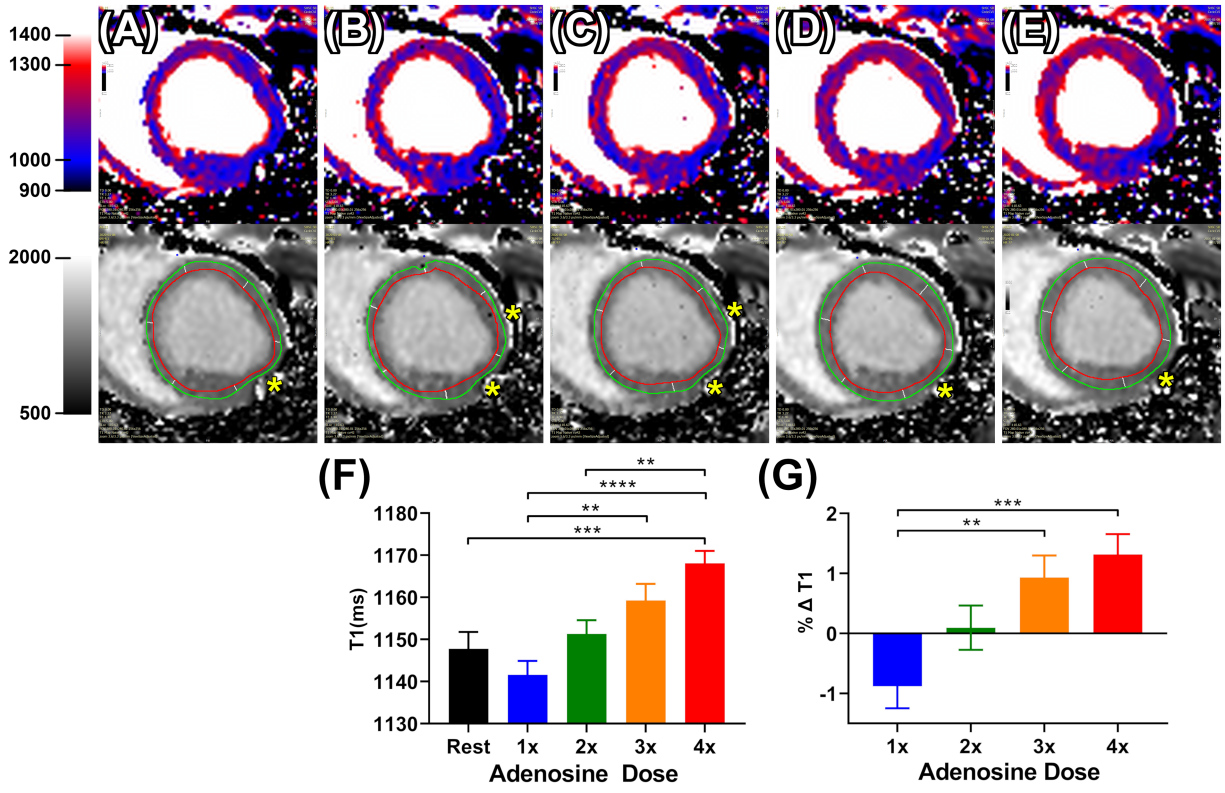

FIGURE 5 Myocardial T1 increases in response to higher adenosine. A-E, T1 maps of the same heart slice at rest (A) and during adenosine infusions at a 1× (B), 2× (C), 3× (D) and 4× (E) doses both without (top) and with (bottom) contours. Pixels are false-colored as in the keys beside A. Segments containing imaging artifacts (yellow asterisks) were excluded from analysis. F, G, Quantification of stress T1 (F) and percent change in stress T1 (G). Colored bars represent the average of myocardial segments

TABLE 2 Results of multivariable linear regression analyses

	Change from rest				Change from next-lowest dose		
	Rest to 1×	Rest to 2×	Rest to 3×	Rest to 4×	1× to 2×	2× to 3×	3× to 4×
Model R^2	0.63	0.48	0.22	0.25	0.71	0.36	0.37
MBF β	**9.48**	**7.03**	0.04	0.36	**7.07**	0.26	−1.54
P-value	**<0.0001**	**0.001**	0.971	0.273	**0.002**	0.816	0.208
O_2 consumption β	0.00041	−0.00010	**−0.00095**	−0.00063	0.00010	**−0.00245**	0.00007
P-value	0.215	0.814	**0.023**	2.216	0.901	**0.004**	0.813
MBV β	−0.023	0.003	0.002	0.024	0.036	−0.008	−0.016
P-value	0.097	0.843	0.906	1.153	0.119	0.715	0.367

Statistically significant β values are bolded.

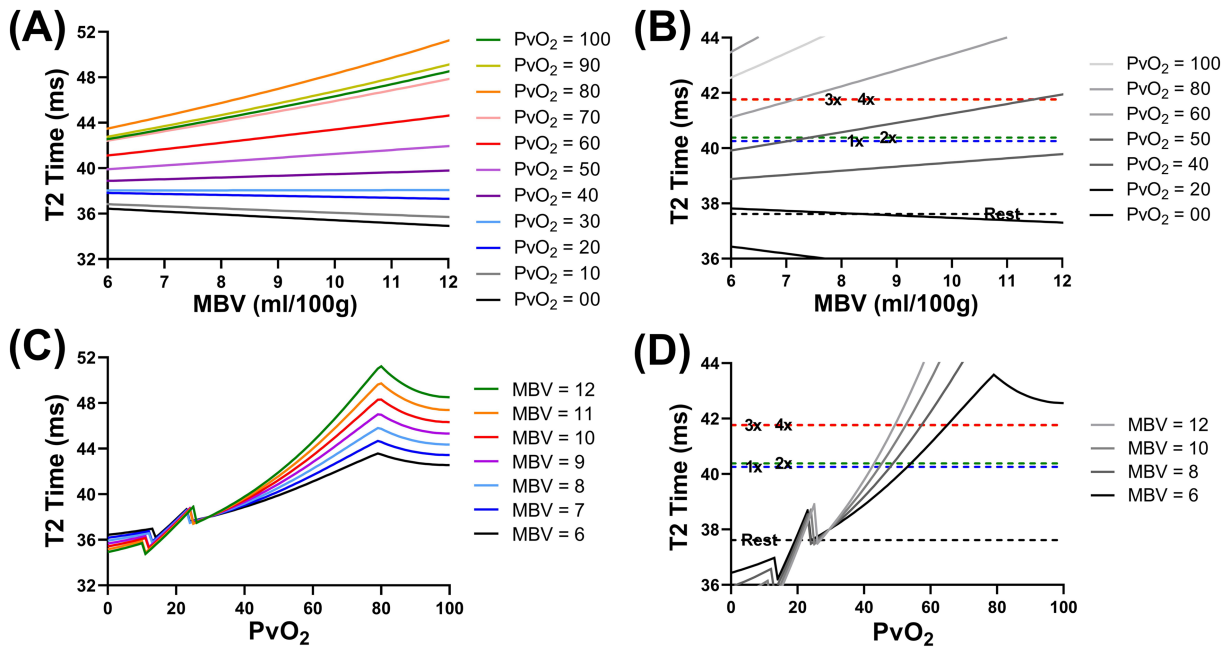

FIGURE 6 Simulations reveal that stress T2 is more affected by changes in PvO_2 than MBV. A, Simulations modeling how stress T2 would be affected if only MBV changed while the PvO_2 was held steady. Each line represents a simulation with a different constant PvO_2. B, Magnification of A with our experimental results overlaid (dotted lines). There is no simulation that intersects with all experimental values. C, Simulations modeling how stress T2 would be affected if only the PvO_2 changed while MBV was held constant. Each line represents a simulation with a different constant MBV. D, Magnification of C with our experimental results overlaid (dotted lines). All simulations intersect with all experimental values

large changes in MBV had a small effect on T2, unless PvO_2 was high (Figure 6A, Table 3). Furthermore, comparing simulation results with experimental results revealed that no single simulation was capable of accounting for all our measured T2 values (Figure 6B). Thus, changing MBV in response to adenosine stress without also changing PvO_2 is not physiologically realistic.

We then ran simulations holding the MBV constant to determine how PvO_2 independently affects stress T2. These simulations revealed that small changes in PvO_2 had a large effect on T2 (Figure 6C, Table 4). Interestingly, altering the level of MBV held constant had little effect when PvO_2 was less than 50%, in agreement with the previous simulation. Overlaying our experimentally derived T2 values showed that every simulation would be able to account for our data through changes in PvO_2 alone (Figure 6D). As such, changing PvO_2 without changing MBV is physiologically feasible, as occurs during intracoronary adenosine infusion.[16,39,46] Overall, these simulations demonstrate that stress-induced changes in PvO_2 have a much bigger influence on stress T2 than do changes in MBV.

TABLE 3 Selected stress T2 values (ms) from simulations varying MBV with constant PvO_2

	MBV = 8	MBV = 12	% ΔMBV
$PvO_2 = 20$	37.65	37.31	−0.91
$PvO_2 = 50$	40.58	41.95	3.37
$PvO_2 = 80$	45.75	51.23	11.99

Results represent a 50% increase in MBV, the high end of what is physiologically possible.

TABLE 4 Selected stress T2 values (in ms) from simulations varying PvO_2 with constant MBV

	$PvO_2 = 20$	$PvO_2 = 80$	% ΔPvO_2
MBV = 6	37.82	43.49	14.99
MBV = 9	37.56	46.98	25.07
MBV = 12	37.31	51.23	37.33

4 | DISCUSSION

To the best of our knowledge, this study was the first to evaluate MBF and oxygen consumption (as components of PvO_2) and MBV during differing levels of hyperemic stress to determine their individual contributions to stress T2. Multivariable analyses revealed MBF as the most influential factor, and T2 simulations agreed that PvO_2 was stronger than MBV. Together, our results indicate several patterns that can be used to build a more comprehensive model of stress T2 sensitivity.

4.1 | A model of myocardial adenosine stress T2 sensitivity

Changes in myocardial oxygen consumption were consistently shown to have minimal influence on stress T2; multivariable analyses gave β-values smaller than 0.002 (Table 2), and the largest incremental change in oxygen consumption (at the 2× dose) failed to induce a noticeable change in T2 (Table 5). In addition, despite oxygen consumption being a component of PvO_2, its patterns of incremental change did not match the simulation predictions for PvO_2 (Table 5, Figure 6). As such, we conclude that changes in myocardial oxygen consumption do not influence adenosine stress T2. Therefore, since PvO_2 is affected by both oxygen consumption and MBF, any adenosine-induced changes in PvO_2 detected by stress T2 can be considered to be due to changes in MBF. With this revelation, simulation results (which implicated PvO_2 as the strongest factor) and multivariable analyses (which indicated MBF) both point to a model where MBF is the most influential factor determining stress T2.

Interestingly, multivariable analyses suggest that the effect of MBF wanes at high levels of hyperemia (Table 2), a shift that can be confirmed with careful observation of the incremental changes between adenosine doses. The 1× dose of adenosine induced the largest incremental increase in stress T2, yet physiologically only MBF changed at the 1× dose in a way that would be expected to increase T2; the change in MBV at

TABLE 5 Summary of hemodynamic changes induced by each dose of adenosine, compared with their effect on stress T2

	Changes from Rest				Incremental Changes (from Next-Lowest Dose)			
	Rest to 1x	Rest to 2x	Rest to 3x	Rest to 4x	Rest to 1x	1x to 2x	2x to 3x	3x to 4x
T2 (ms)	2.64	2.76	**4.15**	**4.16**	**2.64**	0.12	1.39	0.01
MBF (ml/min/g)	0.35	0.48	**0.84**	0.46	**0.35**	0.13	**0.36**	**-0.38**
RPP (bmp * mmHg)	396.00	-797.00	-1805.00	**-2506.00**	396.00	**-1193.00**	-1008.00	-701.00
T1 (ms)	-6.15	3.55	11.45	**20.28**	-6.15	**9.70**	7.90	8.83
MPR	1.44	2.18	**3.10**	2.59	**1.44**	0.74	0.92	-0.51

Numbers represent the change in each component from either rest or the next-lowest dose, as specified. Green highlighting means the change would increase T2, while red indicates a decrease. When compared with rest, bolded values represent the point of highest change. When compared with the next-lowest adenosine dose, bolded values demarcate the greatest step-wise change, with multiple bolded values indicating changes of similar magnitude. Comparing the overall patterns of change exhibited by each factor with that of stress T2 reveals MBF as the most similar to T2, though it alone cannot fully account for the stress T2 pattern.

this dose should decrease T2 (Table 5). Therefore, MBF clearly had a strong influence on T2 at the 1× dose, as it balanced out a negative change in MBV to still induced an increase in T2. Yet at the 3× and 4× doses, MBF changes of similar magnitude to the change at the 1× dose were unable to induce equally strong shifts in T2 (Table 5). Thus, while MBF is the strongest factor, it must be weaker at high levels of hyperemia.

Our modeling for MBV, however, had some inconsistencies. While multivariable analyses suggested MBV only had small effects on stress T2 (Table 2), none of the associated β-values reached significance, bringing this conclusion into question. A closer study of the incremental changes between each dose suggests otherwise; at the 4× dose, changes in MBF and MBV that should cause opposite effects on T2 did indeed balance each other out to result in no change in T2 (Table 5), indicating that MBV must have had an impact at this high level of hyperemia. Simulation results agreed, predicting that MBV's effect increases at higher PvO_2 (Figure 6), which corresponds to high hyperemia. Therefore, we conclude that MBV has an effect on adenosine stress T2 at high levels of hyperemia.

Taken collectively, the above data allow us to build an overall model of the adenosine stress T2 response within the myocardium (Figure 7). While T2 is sensitive to PvO_2, MBF, myocardial oxygen consumption, and MBV, the changes in each of these factors induced by adenosine-based hyperemia do not equally feed into the observed changes in T2. At low hyperemia T2 is most sensitive to changes in MBF, while at high hyperemia T2 responds to changes in both MBF and MBV (Figure 7). Myocardial oxygen consumption has almost no effect on stress T2.

Our overall model agrees with a recent study by Nickander et al., who similarly found that the main hemodynamic factors affecting T2 during adenosine stress in humans are MBF and MBV; RPP also failed to correlate with T2 in their results.[29] While the lack of an effect due to decreased RPP is unexpected, Le et al. found that changes in HR only induce mild effects in oxygen consumption if cardiac contractility does not change.[47] While we did not measure contractility, it is conceivable that the parallel decreases in HR and BP we observed would not alter contractility.

4.2 | Systemic responses to adenosine

Wilson et al. reported that maximal myocardial response to intravenously infused adenosine is achieved within <90 s in humans.[35] Our observations in pigs agree, where much of the effect of adenosine, measured by HR, BP, and RPP, was obtained in the first minute of the adenosine infusion (Figure 4A and Supporting Figure 2A,C,D). In pigs, however, after this initial rapid change, the drop in hemodynamics slowed but BP, HR, and RPP continued to drop during the entire adenosine infusion (Supporting Figure S1), suggesting continued change in all hyperemic effects. Since T1, T2, and microsphere injections are taken at single time points, this warns against assuming that hyperemic stress levels are the same at each measurement, as hyperemia is not the same at the end of a long adenosine infusion as at the beginning. Because of this continued change, strict timing after the start of infusion was enacted for each measurement to ensure consistency. While our 2 min lead time for adenosine infusion measurements is shorter than the 3-4 min used in many other studies, our data support the notion that 2 min was sufficient for the adenosine effect to be established (Figure 4A and Supporting Figure 2A,C,D).

It is interesting to note that in humans adenosine stress increases HR,[29,48–50] but pre-clinically some studies report a decrease[8,51] similar to ours (Supporting Figure 2D,E), while others describe an increase.[5,50,52] This difference is not species specific, but instead may be caused by the anesthesia: studies using injectable anesthetics describe increased HR, while studies using inhaled anesthesia report a decrease in HR. Despite this differing HR response, our study suggests that HR, as a component of RPP, and therefore oxygen consumption, does not greatly impact stress T2 (Figure 7). Indeed, studies documenting increases in RPP (opposite to our study) still report comparable increases in stress T2.[29,50]

4.3 | Adenosine as a hyperemic stress agent

While our study focused on adenosine-based hyperemia, other pharmacologic agents can also be used for stress imaging, though they may act via differing biological mechanisms. For example, dobutamine induces systemic vasodilation, but it also has a direct inotropic effect on the heart,

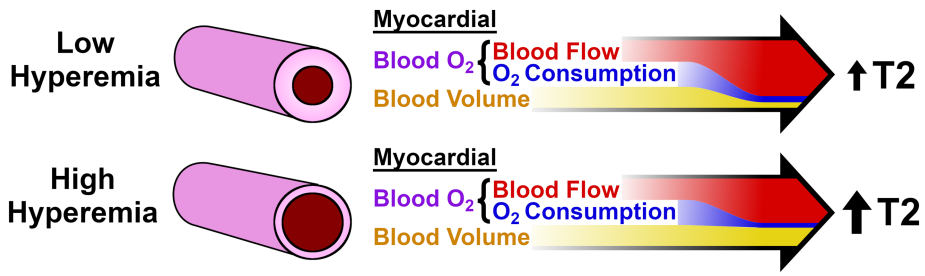

FIGURE 7 Model of myocardial adenosine stress T2 sensitivity. MBF is the dominant factor at all levels of hyperemic stress, but MBV increases its influence at high hyperemia. Oxygen consumption has minimal influence on stress T2

increasing both cardiac output and myocardial oxygen consumption. Even adenosine-related agents can have a different mechanistic basis; regadenoson is specific to the A_{2A} adenosine receptor.[53] These differing mechanistic bases would induce hemodynamic profiles different from that induced by adenosine. As such, we caution against expanding our conclusions to hyperemia induced with vasoactors other than adenosine.

Previous pig studies by various groups used adenosine for stress imaging at doses ranging from 0.14 to 0.50 mg/kg/min,[5,7,8,52,54] all to differing hyperemic effects, making dose considerations and hyperemic expectations difficult to predict. Our study has clarified this; both the 3× and 4× doses of adenosine induce maximal hyperemia in Yorkshire pigs, with peak MBF at the 3× dose (Figure 3), and peak MBV at the 4× dose (Figure 5).

While it is surprising that MBF decreased at the highest dose of adenosine, other groups have observed a similar reversal.[8] Mechanistically, this may be due to saturation or delayed activation of specific adenosine receptor subtypes within the myocardium, shifting the predominant downstream effector; indeed, the vasodilatory action of the A_{2A} and A_{2B} adenosine receptors is opposed by activation of the A_1 and A_3 receptor subtypes.[55] This may also account for the continued trends of systemic measurements (BP, HR, RPP) through the 4× adenosine dose, as each organ has differing ratios of each receptor.[56] Additionally, the continued increase in MBV after MBF begins to drop can be explained by the recent findings of Shah et al., who found that adenosine-induced changes in MBF and MBV are controlled by different adenosine receptors: MBF via the A_{2A} adenosine receptor, and MBV through both the A_{2A} and A_{2B} receptor subtypes.[57] We should also point out that, since the distribution of each adenosine receptor subtype varies from species to species,[56] it is possible that our model may need to be adjusted for stress imaging studies in other species.

4.4 | MBV and MBF measurements

Our study used stress T1 imaging to determine changes in MBV. While this is an accepted method of measuring MBV,[58] it does not provide a direct measurement, but instead provides a value that can be compared between two states (e.g. rest and stress) to obtain the change in MBV. A more direct assay for MBV would have been ideal. However, even though MBV can be non-invasively measured using quantitative first pass perfusion CMR,[59] this technique was not feasible with our experimental design due to its reliance on a gadolinium-based contrast agent. The serum half-life of most gadolinium-based agents is approximately 70-90 min,[60,61] yet our study would have required five injections per CMR examination (during rest and four adenosine doses), raising concerns of incomplete washout between doses and decreased accuracy with later measurements. Therefore, we chose to use contrast-free stress T1 mapping to determine the change in MBV.

We note that, while our resting T1 values are in line with those from other studies done on a 3 T system,[26,62] our changes in T1 from rest to stress (1.3% at the 4× adenosine dose, Table 1) are lower than what others have reported (2.8-6.2%).[26,29,49] Similarly, when using a conversion factor derived from Nickander et al., where a 34.4% change in MBV corresponded to a 6.2% change in T1,[29] our measured T1 values equate to an MBV increase of 7.31% at the 4× adenosine dose (Table 6), whereas other studies using systemic adenosine infusion reported increases of 30-34%.[29,52] This difference may be in part due to the vasodilatory action of isoflurane, which would reduce the effect of adenosine.[63,64] It is also possible that the conversion factor, calculated from measurements in humans, may not transfer to anesthetized pigs.

Regardless of the uncertainties outlined above, the decrease in MBV at the 1× dose was unexpected (Figure 5). The same adenosine dose increased MBF (Figure 3), but a corresponding decrease in MBV suggests a derecruitment of myocardial capillaries. This is likely driven by coronary autoregulatory mechanisms that balance small changes in blood oxygen by adjusting the capillary bed size.[47,65]

Microspheres are widely accepted as the gold standard for MBF measurements[40,41]; however, our microsphere-based MBF values were lower than those reported in other large animal studies that measured MBF via microspheres (Supporting Table).[6,52,59] We used standard microsphere processing techniques and calculations,[40,41] but cannot exclude experimental biases or systematic errors that may have led to skewed results. Regardless, our corresponding MPR values are similar to those reported by other studies,[6,52,59] suggesting that the MBF values are accurate in relation to each other.

Both our T1 and T2 values were similar to those reported by other groups using a 3 T system.[26,50,62] While we did not make reproducibility measurements in this study, T1 and T2 measures as made by our group have been shown to be reproducible[33,37,66–69]: rest T1 values were in the range 1148-1230 ± 45.97 with a coefficient of variation (CV) of 0.038, and rest T2 values in the range 36.5-39.8 ± 1.38 with a CV of 0.036.

TABLE 6 Conversion of change in T1 to change in MBV

Adenosine dose	T1% Δ	Equivalent % Δ in MBV
1×	−0.88	−4.91
2×	0.10	0.56
3×	0.93	5.19
4×	1.31	7.31

We also note that we did not re-measure resting values of T2, MBF, and MBV between each dose of adenosine. (HR and BP records, on the other hand, were restarted prior to the start of each adenosine infusion, giving new rest values for each round.) MBF measurements were limited by the number of microsphere colors with distinct spectral profiles that we could use per pig, such that we would have had to double the number of animals to obtain microsphere-based resting values for each adenosine dose. T1 and T2 scans were also not done between adenosine doses to avoid lengthening what were already long scan times. Since hemodynamic responses generally decrease slightly over the duration of anesthetization, some of our values were likely artificially altered slightly by being compared with rest values not obtained immediately before acquisition. However, since dose administration was randomized, this effect should have been spread across all doses.

4.5 | Stress T2 mapping compared with other stress imaging techniques

The ability of stress T2 to detect both MBF and MBV at high hyperemia puts T2 on par with other stress imaging techniques that also measure both factors, such as first pass perfusion CMR[59] and myocardial contrast echocardiography.[16] The ability to detect both MBF and MBV also indicates that stress T2 is sensitive to changes within different regions of the coronary tree, since MBF is most affected by arterioles and small vessels,[70,71] and MBV changes via capillary recruitment.[72] Therefore, stress T2 provides similar physiological information to contrast-based stress imaging options, but it is contrast free.

There is, however, another emerging option for stress imaging that is also non-contrast: stress T1 mapping. T1 is a CMR-based technique sensitive to tissue fluid levels that can provide information on extracellular volume, MBV, and fibrosis.[73] However, while T1 mapping can identify edematous[34,45] or infarcted[34,74–76] myocardium without stress, stress induction is needed to detect ischemic regions. Stress T1 mapping can detect changes in MBV, but unfortunately it is not sensitive to MBF, RPP, or PvO_2,[26,73] suggesting that T2 is more sensitive to the underlying hemodynamic effects. Stress T1 also suffers from a narrow dynamic range that has plagued attempts to identify ischemic or infarcted myocardium; even in healthy remote myocardium, the rest-stress percent change measured using T1 is 6% or less,[26,29,77–79] as compared with a more than 10% change detected using T2.[29,50] Additionally, while some studies report being able to differentiate ischemic or infarcted tissue from healthy myocardium using stress T1, they only do so successfully when the regions are previously demarcated by perfusion or late gadolinium imaging[77,79]; differentiation by stress T1 alone, when blinded to the location of the ischemia, fails.[77] These underlying uncertainties make stress T1 imaging a less attractive non-contrast option for the identification of ischemic myocardium than stress T2.

4.6 | Clinical implications

This study demonstrates the potential for stress T2 mapping to be a non-contrast stress imaging option for the identification of ischemic myocardium. While more work is needed to confirm the clinical accuracy of stress T2 imaging in humans, the predictive power of stress imaging with other imaging techniques[9,10] hints at the role that stress T2 imaging may play in a clinical setting. Importantly, the non-contrast nature of stress T2 removes the risks of repeated imaging, enabling the possible utility of stress T2 mapping in routine screening. This would allow for much earlier detection and intervention in those at risk of heart disease, but could also provide a critical first indication of disease for asymptomatic patients.

Our study also indicates that varying hyperemia can be used to gain additional insights into the state of the myocardium: low hyperemia reveals the changes in MBF, while high hyperemia uncovers the changes in MBF and MBV combined. Since MBF and MBV are regulated in different regions of the coronary tree,[70–72] stress T2 could provide a single imaging technique to probe the vasoactivity of different vessel types. While the adenosine doses used to establish low and high hyperemia in Yorkshire pigs likely do not translate to humans, human studies evaluating the use of adenosine doses higher[80,81] and lower[35,82] than the "standard" dose of 0.14 mg/kg/min demonstrate that there is a range of efficacy that could be further explored for this purpose.

4.7 | Limitations

There are several limitations related to our study design. First was the use of isoflurane as the anesthetic. In addition to the aforementioned potential reversal to the expected change in HR, isoflurane has multiple effects on the cardiovascular system.[83] Of greatest concern, it is a vasodilator,[63,64,84] albeit a much weaker one than adenosine: 3% isoflurane produces a 10-fold lower increase in coronary blood flow than adenosine (a 51% versus a 591% increase, respectively).[84] Nevertheless, these effects would decrease vasodilator-induced hyperemia. To limit this, isoflurane doses between 2 and 3.5% were used during the relevant coronary hemodynamic measurements. Second, as mentioned above, we used stress T1 mapping to correlate to changes in MBV, rather than measuring MBV directly. Third, the microsphere injections and CMR scans were done on different days, introducing possible inconsistencies. Fourth, we did not re-measure resting values of MBV and MBF between each dose of adenosine.

Another study limitation was brought to light in a recent paper, where Yang et al. demonstrated that high HR (>100 bpm) causes artificially low T2 values, which then require an HR correction.[50] Our average baseline HR was 99, so many of our T2 values needed this correction; however, the correction requires a change in scan parameters, and therefore was not applied in our study.

5 | FINAL CONCLUSIONS

To the best of our knowledge, this is the first study to determine the effects of adenosine-based hyperemic stress at varying levels in order to better understand what physiological changes within the myocardium have the biggest individual impact on stress T2. Our results point to MBF as the largest driving factor behind changes in adenosine stress T2, though MBV also plays a role at high hyperemia. Oxygen consumption has minimal effect. Overall, these results clarify how changes in stress T2 can be interpreted in terms of the physiological changes that happen during hyperemic stress. With this improved understanding, stress T2 mapping becomes a promising, non-invasive, non-contrast option for detecting ischemic myocardium.

ACKNOWLEDGEMENTS

We thank Nitish Bhatt for help with T1 metadata handling, Idan Roifman for assistance with the multivariable analysis, and Calder Sheagren for facilitating the microsphere analysis calculations.

This study was supported with funding from the National Institutes of Health, USA (NIH-RO1-5R01HL130494-04), the Ontario Research Fund, Canada (ORF-RE7-21), and the Heart and Stroke Foundation of Ontario (HSFO) (grant-in-aid G-18-0020475). Dr Ghugre is also supported by the National New Investigator (NNI) award from the Heart and Stroke Foundation of Canada (HSFC).

DATA AVAILABILITY STATEMENT

The data that support the findings of this study are available from the corresponding author upon reasonable request.

ORCID

Jill J. Weyers https://orcid.org/0000-0003-2358-1162
Ahsan Javed https://orcid.org/0000-0003-1311-1247
Krishna Nayak https://orcid.org/0000-0001-5735-3550
Nilesh R. Ghugre https://orcid.org/0000-0002-5395-1956

REFERENCES

1. Friedman M, Spalding J, Kothari S, Wu Y, Gatt E, Boulanger L. Myocardial perfusion imaging laboratory efficiency with the use of regadenoson compared to adenosine and dipyridamole. *J Med Econ*. 2013;16(4):449-460. https://doi.org/10.3111/13696998.2013.772057
2. Brana Q, Thibault F, Courtehoux M, et al. Regadenoson versus dipyridamole: evaluation of stress myocardial blood flow response on a CZT-SPECT camera. *J Nucl Cardiol*. 2020. https://doi.org/10.1007/s12350-020-02271-5
3. Johnston DL, Daley JR, Hodge DO, Hopfenspirger MR, Gibbons RJ. Hemodynamic responses and adverse effects associated with adenosine and dipyridamole pharmacologic stress testing: a comparison in 2,000 patients. *Mayo Clin Proc*. 1995;70(4):331-336. https://doi.org/10.4065/70.4.331
4. Martin TW, Seaworth JF, Johns JP, Pupa LE, Condos WR. Comparison of adenosine, dipyridamole, and dobutamine in stress echocardiography. *Ann Intern Med*. 1992;116(3):190-196. https://doi.org/10.7326/0003-4819-116-3-190
5. Rossi A, Uitterdijk A, Dijkshoorn M, et al. Quantification of myocardial blood flow by adenosine-stress CT perfusion imaging in pigs during various degrees of stenosis correlates well with coronary artery blood flow and fractional flow reserve. *Eur Heart J Cardiovasc Imaging*. 2013;14(4):331-338. https://doi.org/10.1093/ehjci/jes150
6. Bamberg F, Hinkel R, Schwarz F, et al. Accuracy of dynamic computed tomography adenosine stress myocardial perfusion imaging in estimating myocardial blood flow at various degrees of coronary artery stenosis using a porcine animal model. *Invest Radiol*. 2012;47(1):71-77. https://doi.org/10.1097/RLI.0b013e31823fd42b
7. Schwarz F, Hinkel R, Baloch E, et al. Myocardial CT perfusion imaging in a large animal model: comparison of dynamic versus single-phase acquisitions. *JACC Cardiovasc Imaging*. 2013;6(12):1229-1238. https://doi.org/10.1016/j.jcmg.2013.05.018
8. Van Houten M, Yang Y, Hauser A, et al. Adenosine stress CMR perfusion imaging of the temporal evolution of perfusion defects in a porcine model of progressive obstructive coronary artery occlusion. *NMR Biomed*. 2019;32(11):1-11. https://doi.org/10.1002/nbm.4136
9. Knott KD, Seraphim A, Augusto JB, et al. The prognostic significance of quantitative myocardial perfusion: an artificial intelligence-based approach using perfusion mapping. *Circulation*. 2020;141(16):1282-1291. https://doi.org/10.1161/CIRCULATIONAHA.119.044666
10. Luong TV, Pedersen MGB, Kjærulff MLBG, et al. Ischemic heart failure mortality is not predicted by cardiac insulin resistance but by diabetes perse and coronary flow reserve: a retrospective dynamic cardiac 18F-FDG PET study. *Metabolism*. 2021;123:154862. https://doi.org/10.1016/j.metabol.2021.154862
11. Al-Saadi N, Nagel E, Gross M, et al. Noninvasive detection of myocardial ischemia from perfusion reserve based on cardiovascular magnetic resonance. *Circulation*. 2000;101(12):1379-1383. https://doi.org/10.1161/01.CIR.101.12.1379

12. Dorbala S, Di Carli MF, Beanlands RS, et al. Prognostic value of stress myocardial perfusion positron emission tomography: results from a multicenter observational registry. *J Am Coll Cardiol*. 2013;61(2):176-184. https://doi.org/10.1016/j.jacc.2012.09.043
13. Fukushima K, Javadi MS, Higuchi T, et al. Prediction of short-term cardiovascular events using quantification of global myocardial flow reserve in patients referred for clinical 82Rb PET perfusion imaging. *J Nucl Med*. 2011;52(5):726-732. https://doi.org/10.2967/jnumed.110.081828
14. Bastarrika G, Ramos-Duran L, Rosenblum MA, Kang DK, Rowe GW, Schoepf UJ. Adenosine-stress dynamic myocardial CT perfusion imaging: initial clinical experience. *Invest Radiol*. 2010;45(6):306-313. https://doi.org/10.1097/RLI.0b013e3181dfa2f2
15. Blankstein R, Shturman LD, Rogers IS, et al. Adenosine-induced stress myocardial perfusion imaging using dual-source cardiac computed tomography. *J Am Coll Cardiol*. 2009;54(12):1072-1084. https://doi.org/10.1016/j.jacc.2009.06.014
16. Wei K, Jayaweera AR, Firoozan S, Linka A, Skyba DM, Kaul S. Quantification of myocardial blood flow with ultrasound-induced destruction of microbubbles administered as a constant venous infusion. *Circulation*. 1998;97(5):473-483. https://doi.org/10.1161/01.CIR.97.5.473
17. Grobner T. Gadolinium—a specific trigger for the development of nephrogenic fibrosing dermopathy and nephrogenic systemic fibrosis? *Nephrol Dial Transplant*. 2006;21(4):1104-1108. https://doi.org/10.1093/ndt/gfk062
18. Hausleiter J, Meyer T, Hermann F, et al. Estimated radiation dose associated with cardiac CT angiography. *J Am Med Assoc*. 2009;301(5):500-507. https://doi.org/10.1001/jama.2009.54
19. Desiderio MC, Lundbye JB, Baker WL, Farrell MB, Jerome SD, Heller GV. Current status of patient radiation exposure of cardiac positron emission tomography and single-photon emission computed tomographic myocardial perfusion imaging. *Circ Cardiovasc Imaging*. 2018;11(12):e007565. https://doi.org/10.1161/CIRCIMAGING.118.007565
20. Gibby WA, Gibby KA, Gibby WA. Comparison of Gd DTPA-BMA (Omniscan) versus Gd HP-DO3A (ProHance) retention in human bone tissue by inductively coupled plasma atomic emission spectroscopy. *Invest Radiol*. 2004;39(3):138-142. https://doi.org/10.1097/01.rli.0000112789.57341.01
21. White GW, Gibby WA, Tweedle MF. Comparison of Gd (DTPA-BMA) (Omniscan) versus Gd (HP-DO3A) (ProHance) relative to gadolinium retention in human bone tissue by inductively coupled plasma mass spectroscopy. *Invest Radiol*. 2006;41(3):272-278. https://doi.org/10.1097/01.rli.0000186569.32408.95
22. McDonald RJ, McDonald JS, Kallmes DF, et al. Intracranial gadolinium deposition after contrast-enhanced MR imaging. *Radiology*. 2015;275(3):772-782. https://doi.org/10.1148/radiol.2015150697
23. Kanda T, Fukusato T, Matsuda M, et al. Gadolinium-based contrast agent accumulates in the brain even in subjects without severe renal dysfunction: evaluation of autopsy brain specimens with inductively coupled plasma mass spectroscopy. *Radiology*. 2015;276(1):228-232. https://doi.org/10.1148/radiol.2015142690
24. Bauer WR, Nadler W, Bock M, et al. The relationship between the BOLD-induced T_2 and T_2^*: a theoretical approach for the vasculature of myocardium. *Magn Reson Med*. 1999;42(6):1004-1010. https://doi.org/10.1002/(SICI)1522-2594(199912)42:6<1004::AID-MRM2>3.0.CO;2-M
25. Stainsby JA, Wright GA. Monitoring blood oxygen state in muscle microcirculation with transverse relaxation. *Magn Reson Med*. 2001;45(4):662-672. https://doi.org/10.1002/mrm.1089
26. Mahmod M, Piechnik SK, Levelt E, et al. Adenosine stress native T1 mapping in severe aortic stenosis: evidence for a role of the intravascular compartment on myocardial T1 values. *J Cardiovasc Magn Reson*. 2014;16(1):92. https://doi.org/10.1186/s12968-014-0092-y
27. Ogawa S, Lee TM, Nayak AS, Glynn P. Oxygenation-sensitive contrast in magnetic resonance image of rodent brain at high magnetic fields. *Magn Reson Med*. 1990;14(1):68-78. https://doi.org/10.1002/mrm.1910140108
28. Ogawa S, Lee TM, Kay AR, Tank DW. Brain magnetic resonance imaging with contrast dependent on blood oxygenation. *Proc Natl Acad Sci U S A*. 1990;87(24):9868-9872. https://doi.org/10.1073/pnas.87.24.9868
29. Nickander J, Themudo R, Thalén S, et al. The relative contributions of myocardial perfusion, blood volume and extracellular volume to native T1 and native T2 at rest and during adenosine stress in normal physiology. *J Cardiovasc Magn Reson*. 2019;21(1):73. https://doi.org/10.1186/s12968-019-0585-9
30. Wright KB, Klocke FJ, Deshpande VS, et al. Assessment of regional differences in myocardial blood flow using T_2-weighted 3D BOLD imaging. *Magn Reson Med*. 2001;46(3):573-578. https://doi.org/10.1002/mrm.1229
31. Fieno DS, Shea SM, Li Y, Harris KR, Finn JP, Li D. Myocardial perfusion imaging based on the blood oxygen level-dependent effect using T_2-prepared steady-state free-precession magnetic resonance imaging. *Circulation*. 2004;110(10):1284-1290. https://doi.org/10.1161/01.CIR.0000140673.13057.34
32. Wright GA, Hu BS, Macovski A. Estimating oxygen saturation of blood in vivo with MR imaging at 1.5 T. *J Magn Reson Imaging*. 1991;1(3):275-283. https://doi.org/10.1002/jmri.1880010303
33. Ghugre NR, Ramanan V, Pop M, et al. Myocardial BOLD imaging at 3 T using quantitative T_2: application in a myocardial infarct model. *Magn Reson Med*. 2011;66(6):1739-1747. https://doi.org/10.1002/mrm.22972
34. Ugander M, Bagi PS, Oki AJ, et al. Myocardial edema as detected by pre-contrast T1 and T2 CMR delineates area at risk associated with acute myocardial infarction. *JACC Cardiovasc Imaging*. 2012;5(6):596-603. https://doi.org/10.1016/j.jcmg.2012.01.016
35. Wilson RF, Wyche K, Christensen BV, Zimmer S, Laxson DD. Effects of adenosine on human coronary arterial circulation. *Circulation*. 1990;82(5):1595-1606. https://doi.org/10.1161/01.CIR.82.5.1595
36. Kellman P, Hansen MS. T1-mapping in the heart: accuracy and precision. *J Cardiovasc Magn Reson*. 2014;16(1):2. https://doi.org/10.1186/1532-429X-16-2
37. Assimopoulos S, Shie N, Ramanan V, et al. Hemorrhage promotes chronic adverse remodeling in acute myocardial infarction: a T_1, T_2 and BOLD study. *NMR Biomed*. 2021;34(1):e4404. https://doi.org/10.1002/nbm.4404
38. Cerqueira MD, Weissman NJ, Dilsizian V, et al. Standardized myocardial segmentation and nomenclature for tomographic imaging of the heart: a statement for healthcare professionals from the Cardiac Imaging Committee of the Council on Clinical Cardiology of the American Heart Association. *Circulation*. 2002;105(5):539-542. https://doi.org/10.1067/mje.2002.123374
39. Foltz WD, Huang H, Fort S, Wright GA. Vasodilator response assessment in porcine myocardium with magnetic resonance relaxometry. *Circulation*. 2002;106(21):2714-2719. https://doi.org/10.1161/01.CIR.0000039475.66067.DC
40. Glenny RW, Bernard S, Brinkley M. Validation of fluorescent-labeled microspheres for measurement of regional organ perfusion. *J Appl Physiol*. 1993;74(5):2585-2597.
41. Glenny RW Fluorescent Microsphere Resource Center. 2019. http://fmrc.pulmcc.washington.edu/. Accessed June 1, 2018.

42. Gould KL, Lipscomb K, Hamilton GW. Physiologic basis for assessing critical coronary stenosis. Instantaneous flow response and regional distribution during coronary hyperemia as measures of coronary flow reserve. *Am J Cardiol*. 1974;33(1):87-94. https://doi.org/10.1016/0002-9149(74)90743-7
43. Goldstein RA, Kirkeeide RL, Demer LL, et al. Relation between geometric dimensions of coronary artery stenoses and myocardial perfusion reserve in man. *J Clin Invest*. 1987;79(5):1473-1478. https://doi.org/10.1172/JCI112976
44. Gobel FL, Norstrom LA, Nelson RR, Jorgensen CR, Wang Y. The rate-pressure product as an index of myocardial oxygen consumption during exercise in patients with angina pectoris. *Circulation*. 1978;57(3):549-556. https://doi.org/10.1161/01.CIR.57.3.549
45. Ferreira VM, Piechnik SK, Dallarmellina E, et al. Non-contrast T1-mapping detects acute myocardial edema with high diagnostic accuracy: a comparison to T2-weighted cardiovascular magnetic resonance. *J Cardiovasc Magn Reson*. 2012;14(1):42. https://doi.org/10.1186/1532-429X-14-42
46. Crystal GJ, Downey HF, Bashour FA. Small vessel and total coronary blood volume during intracoronary adenosine. *Am J Physiol Heart Circ Physiol*. 1981;10(2):194-201. https://doi.org/10.1152/ajpheart.1981.241.2.h194
47. Le DE, Bin JP, Coggins MP, Wei K, Lindner JR, Kaul S. Relation between myocardial oxygen consumption and myocardial blood volume: a study using myocardial contrast echocardiography. *J Am Soc Echocardiogr*. 2002;15(9):857-863. https://doi.org/10.1067/mje.2002.121275
48. Nickander J, Themudo R, Sigfridsson A, Xue H, Kellman P, Ugander M. Females have higher myocardial perfusion, blood volume and extracellular volume compared to males—an adenosine stress cardiovascular magnetic resonance study. *Sci Rep*. 2020;10(1):10380. https://doi.org/10.1038/s41598-020-67196-y
49. Poli FE, Gulsin GS, March DS, et al. The reliability and feasibility of non-contrast adenosine stress cardiovascular magnetic resonance T1 mapping in patients on haemodialysis. *J Cardiovasc Magn Reson*. 2020;22(1):43. https://doi.org/10.1186/s12968-020-00634-y
50. Yang H-J, Dey D, Sykes J, et al. Heart rate-independent 3D myocardial blood oxygen level-dependent MRI at 3.0 T with simultaneous ^{13}N-ammonia PET validation. *Radiology*. 2020;95:82-93.
51. Waller C, Kahler E, Hiller KH, et al. Myocardial perfusion and intracapillary blood volume in rats at rest and with coronary dilatation: MR imaging in vivo with use of a spin-labeling technique. *Radiology*. 2000;215(1):189-197. https://doi.org/10.1148/radiology.215.1.r00ap07189
52. Jerosch-Herold M, Wilke N, Wang Y, et al. Direct comparison of an intravascular and an extracellular contrast agent for quantification of myocardial perfusion. *Int J Card Imaging*. 1999;15(6):453-464. https://doi.org/10.1023/A:1006368619112
53. Cerqueira MD. The future of pharmacologic stress: selective a_{2a} adenosine receptor agonists. *Am J Cardiol*. 2004;94(2 Suppl 1):33-40. https://doi.org/10.1016/j.amjcard.2004.04.017
54. Mannheim D, Versari D, Daghini E, et al. Impaired myocardial perfusion reserve in experimental hypercholesterolemia is independent of myocardial neovascularization. *Am J Physiol Heart Circ Physiol*. 2007;292(5):H2449-H2458. https://doi.org/10.1152/ajpheart.01215.2006
55. Mustafa SJ, Morrison RR, Teng B, Pelleg A. Adenosine receptors and the heart: role in regulation of coronary blood flow and cardiac electrophysiology. In: Wilson CN, Mustafa SJ, eds. *Adenosine Receptors in Health and Disease. Handbook of Experimental Pharmacology*. Vol. 193. Berlin, Germany: Springer; 2009:161-188.
56. Ho M-F, Rose'Meyer RB. Vascular adenosine receptors; potential clinical applications. *Curr Vasc Pharmacol*. 2013;11(3):327-337. https://doi.org/10.2174/1570161111311030007
57. Shah SA, Reagan CE, French BA, Epstein FH. Molecular mechanisms of adenosine stress T1 mapping. *Circ Cardiovasc Imaging*. 2021;14:e011774. https://doi.org/10.1161/CIRCIMAGING.120.011774
58. Piechnik SK, Neubauer S, Ferreira VM. State-of-the-art review: stress T1 mapping—technical considerations, pitfalls and emerging clinical applications. *Magn Reson Mater Phys Biol Med*. 2018;31(1):131-141. https://doi.org/10.1007/s10334-017-0649-5
59. Wilke N, Kroll K, Merkle H, et al. Regional myocardial blood volume and flow: first-pass MR imaging with polylysine-Gd-DTPA. *J Magn Reson Imaging*. 1995;5(2):227-237. https://doi.org/10.1002/jmri.1880050219
60. Oksendal AN, Hals PA. Biodistribution and toxicity of MR imaging contrast media. *J Magn Reson Imaging*. 1993;3(1):157-165. https://doi.org/10.1002/jmri.1880030128
61. Ersoy H, Rybicki FJ. Biochemical safety profiles of gadolinium-based extracellular contrast agents and nephrogenic systemic fibrosis. *J Magn Reson Imaging*. 2007;26(5):1190-1197. https://doi.org/10.1002/jmri.21135
62. Liu X, Hou JL, Yang ZG, et al. Native T_1 mapping for characterization of acute and chronic myocardial infarction in swine: comparison with contrast-enhanced MRI. *J Magn Reson Imaging*. 2018;47(5):1406-1414. https://doi.org/10.1002/jmri.25871
63. Gamperl AK, Hein TW, Kuo L, Cason BA. Isoflurane-induced dilation of porcine coronary microvessels is endothelium dependent and inhibited by glibenclamide. *Anesthesiology*. 2002;96(6):1465-1471.
64. Gilbert M, Roberts SL, Mori M, Blomberg R, Tinker JH. Comparative coronary vascular reactivity and hemodynamics during halothane and isoflurane anesthesia in swine. *Anesthesiology*. 1988;68(2):243-253. https://doi.org/10.1097/00000542-198802000-00011
65. McCommis KS, Zhang H, Goldstein TA, et al. Myocardial blood volume is associated with myocardial oxygen consumption. An experimental study with cardiac magnetic resonance in a canine model. *JACC Cardiovasc Imaging*. 2009;2(11):1313-1320. https://doi.org/10.1016/j.jcmg.2009.07.010
66. Ghugre NR, Pop M, Barry J, Connelly KA, Wright GA. Quantitative magnetic resonance imaging can distinguish remodeling mechanisms after acute myocardial infarction based on the severity of ischemic insult. *Magn Reson Med*. 2013;70(4):1095-1105. https://doi.org/10.1002/mrm.24531
67. Ghugre NR, Pop M, Thomas R, et al. Hemorrhage promotes inflammation and myocardial damage following acute myocardial infarction: insights from a novel preclinical model and cardiovascular magnetic resonance. *J Cardiovasc Magn Reson*. 2017;19(1):50. https://doi.org/10.1186/s12968-017-0361-7
68. Ghugre NR, Ramanan V, Assimopoulos S, et al. T1 and T2 mapping reveal contribution of hemorrhage in myocardial remodeling following acute myocardial infarction. *J Cardiovasc Magn Reson*. 2016;18(Suppl 1):Q5. https://doi.org/10.1186/1532-429X-18-S1-Q5
69. Ghugre NR, Ramanan V, Pop M, et al. Quantitative tracking of edema, hemorrhage, and microvascular obstruction in subacute myocardial infarction in a porcine model by MRI. *Magn Reson Med*. 2011;66(4):1129-1141. https://doi.org/10.1002/mrm.22855
70. Layland J, Carrick D, Lee M, Oldroyd K, Berry C. Adenosine: physiology, pharmacology, and clinical applications. *JACC Cardiovasc Interv*. 2014;7(6):581-591. https://doi.org/10.1016/j.jcin.2014.02.009
71. Goodwill AG, Dick GM, Kiel AM, Tune JD. Regulation of coronary blood flow. *Compr Physiol*. 2017;7(2):321-382. https://doi.org/10.1002/cphy.c160016
72. Li X, Springer CS, Jerosch-Herold M. First-pass dynamic contrast-enhanced MRI with extravasating contrast reagent: evidence for human myocardial capillary recruitment in adenosine-induced hyperemia. *NMR Biomed*. 2009;22(2):148-157. https://doi.org/10.1002/nbm.1293

73. Moon JC, Messroghli DR, Kellman P, et al. Myocardial T1 mapping and extracellular volume quantification: a Society for Cardiovascular Magnetic Resonance (SCMR) and CMR Working Group of the European Society of Cardiology consensus statement. *J Cardiovasc Magn Reson*. 2013;15(1):92. https://doi.org/10.1186/1532-429X-15-92
74. Wang G, Lee SE, Yang Q, et al. Multicenter study on the diagnostic performance of native-T1 cardiac magnetic resonance of chronic myocardial infarctions at 3T. *Circ Cardiovasc Imaging*. 2020;13:e009894. https://doi.org/10.1161/CIRCIMAGING.119.009894
75. Dastidar AG, Harries I, Pontecorboli G, et al. Native T1 mapping to detect extent of acute and chronic myocardial infarction: comparison with late gadolinium enhancement technique. *Int J Cardiovasc Imaging*. 2019;35(3):517-527. https://doi.org/10.1007/s10554-018-1467-1
76. Cui C, Wang S, Lu M, et al. Detection of recent myocardial infarction using native T1 mapping in a swine model: a validation study. *Sci Rep*. 2018;8(1):7391. https://doi.org/10.1038/s41598-018-25693-1
77. Bohnen S, Prüßner L, Vettorazzi E, et al. Stress T1-mapping cardiovascular magnetic resonance imaging and inducible myocardial ischemia. *Clin Res Cardiol*. 2019;108(8):909-920. https://doi.org/10.1007/s00392-019-01421-1
78. Colbert CM, Le AH, Shao J, et al. Ferumoxytol-enhanced magnetic resonance T1 reactivity for depiction of myocardial hypoperfusion. *NMR Biomed*. 2021;34(7):e4518. https://doi.org/10.1002/nbm.4518
79. van Assen M, van Dijk R, Kuijpers D, Vliegenthart R, Oudkerk M. T1 reactivity as an imaging biomarker in myocardial tissue characterization discriminating normal, ischemic and infarcted myocardium. *Int J Cardiovasc Imaging*. 2019;35(7):1319-1325. https://doi.org/10.1007/s10554-019-01554-4
80. Djordjevic-Dikic AD, Ostojic MC, Beleslin BD, et al. High dose adenosine stress echocardiography for noninvasive detection of coronary artery disease. *J Am Coll Cardiol*. 1996;28(7):1689-1695. https://doi.org/10.1016/S0735-1097(96)00374-9
81. Karamitsos TD, Ntusi NA, Francis JM, Holloway CJ, Myerson SG, Neubauer S. Feasibility and safety of high-dose adenosine perfusion cardiovascular magnetic resonance. *J Cardiovasc Magn Reson*. 2010;12(1):66. https://doi.org/10.1186/1532-429X-12-66
82. Zhou X, Zhi G, Xu Y, Wang J, Yan GH. Estimation of coronary artery stenosis by low-dose adenosine stress real-time myocardial contrast echocardiography: a quantitative study. *Chin Med J*. 2012;125(10):1795-1798. https://doi.org/10.3760/cma.j.issn.0366-6999.2012.10.020
83. Constantinides C, Murphy K. Molecular and integrative physiological effects of isoflurane anesthesia: the paradigm of cardiovascular studies in rodents using magnetic resonance imaging. *Front Cardiovasc Med*. 2016;3(July):23. https://doi.org/10.3389/fcvm.2016.00023
84. Hickey RF, Cason BA, Shubayev I. Regional vasodilating properties of isoflurane in normal swine myocardium. *Anesthesiology*. 1994;80(3):574-581.

SUPPORTING INFORMATION

Additional supporting information may be found in the online version of the article at the publisher's website.

How to cite this article: Weyers JJ, Ramanan V, Javed A, et al. Myocardial blood flow is the dominant factor influencing cardiac magnetic resonance adenosine stress T2. *NMR in Biomedicine*. 2022;35(3):e4643. doi:10.1002/nbm.4643